



## Bistable electrowetting device with non-planar designed controlling electrodes for display applications<sup>\*</sup>

Han ZHANG, Xue-lei LIANG<sup>†‡</sup>

*Key Laboratory for the Physics and Chemistry of Nanodevices, Department of Electronics, Peking University, Beijing 100871, China*

<sup>†</sup>E-mail: liangxl@pku.edu.cn

Received Mar. 19, 2018; Revision accepted May 13, 2018; Crosschecked Sept. 4, 2019

**Abstract:** Bistable electrowetting display (EWD) is a promising low-power electronic paper technology, where power is consumed only during the switching between two stable states; however, it is not required for state maintenance once switched. In this paper, a bistable electrowetting device with non-planar designed controlling electrodes is fabricated by a fully conventional photolithography process. The device has potential for video display applications with a controllable gray scale. The novel electrode design realizes a lower driving voltage and a higher contrast between two stable states than the EWDs with planar electrodes reported previously.

**Key words:** Bistable electrowetting; Non-planar; Controlling electrodes; Low voltage; High contrast

<https://doi.org/10.1631/FITEE.1800167>

**CLC number:** TN27

### 1 Introduction

Electrowetting (EW) is an effect of tuning the contact angle of a liquid droplet to a solid surface by applying an electric field (Jones, 2005; Mugele and Baret, 2005). The contact angle can be tuned over 90° by EW (Lao, 2008) with actuating speeds on the time scale of milliseconds (Hayes and Feenstra, 2003). This capability has made EW the most powerful and popular tool for manipulating tiny amounts of liquids, including generating, moving, merging, splitting, and mixing droplets in microsystems such as digital microfluidic systems (Cho et al., 2003; Huh et al., 2003), adjustable liquid lenses (Kuiper and Hendriks, 2004; Smith et al., 2006; Hou et al., 2007), and lab-on-a-chip devices (Pollack et al., 2002; Huh et al., 2003). Droplets controlled by EW can be used as optical

switches, which have potential for display applications (Hayes and Feenstra, 2003; Heikenfeld et al., 2009; Zhou et al., 2009; Chen et al., 2011; Shui et al., 2014). Therefore, a new kind of display technology, electrowetting display (EWD), has emerged (Heikenfeld et al., 2009; Zhou et al., 2009; Chen et al., 2011; Deng et al., 2017). Compared with the existing display technologies, EWDs have advantages over liquid crystal displays (LCDs), including low power consumption, wide viewing angles, and high brightness which is comparable to that of traditional paper in direct sunlight (Mugele and Baret, 2005; Blankenbach et al., 2011; Deng et al., 2017). EWDs surpass the commercialized electronic paper (e-paper) technologies, such as those based on the electrophoretic technology (Comiskey et al., 1998), in the capability of video speed and full color mode operation (Hayes and Feenstra, 2003; Blankenbach et al., 2008; You and Steckl, 2010). Prototype EWDs have been reported by Blankenbach et al. (2011) and Deng et al. (2017), and commercialization of this new display technology is being actively pursued (Bitman et al., 2012; Jung et al., 2012; Deng et al., 2017). Among the development in current EWDs, the demonstration of a

<sup>‡</sup> Corresponding author

<sup>\*</sup> Project supported by the National Natural Science Foundation of China (No. 61621061) and the National Key R&D Program of China (No. 2016YFA0201902)

ORCID: Xue-lei LIANG, <http://orcid.org/0000-0003-3095-0974>  
 © Zhejiang University and Springer-Verlag GmbH Germany, part of Springer Nature 2019

bistable EWD, in which a droplet in pixels has two stable states, is particularly exciting (Rawert et al., 2010; Yang et al., 2010; Blankenbach et al., 2011; Bitman et al., 2012). Power is consumed only during the switching of pixels; however, it is not required to maintain the pixel states once switched. Thus, the number of times that a pixel needs refreshing in a conventional display (Dai, 2008) is drastically reduced, and less power is needed for bistable display, resulting in a longer battery life. Therefore, bistable EWDs are considered a potential and significant technology for e-paper products.

In bistable EWDs, droplets are confined to either of two distinct stable states, which are electrically switchable (Rawert et al., 2010; Yang et al., 2010; Blankenbach et al., 2011; Bitman et al., 2012). The two confining states of liquids are usually realized by specially designed pixel structures. Thus, a complicated design of the device structure is needed, which causes difficulties in the fabrication process. Because of these challenges, research on bistable EWDs lags far behind that on conventional EWDs. The performance of EWDs is not as good as that of conventional EWDs (Blankenbach et al., 2008). Therefore, efforts are needed to push bistable EWD technology towards commercialization.

Charipar et al. (2015) proposed a bistable EWD, in which planar controlling electrodes were used to manipulate liquid switching out of plane between two stable states. They demonstrated multi-color operation by combining two mono-color pixel layers. In Charipar et al. (2015)'s device fabrication process, a laser-based technique was employed to pattern the planar controlling electrodes, which simplifies the fabrication process. However, this laser patterning process had very low efficiency and the equipment cost for mass production was very high, thus hindering its commercialization. Moreover, there was a very thick dielectric layer with low permittivity between the bottom and top electrodes in Charipar et al. (2015)'s planar electrode design, meaning that a very large operating voltage, about 80–140 V, was needed to switch pixels. Therefore, both the fabrication process and the performance of the device needed improvement.

In this study, a bistable EW device with a non-planar controlling electrode structure is designed and fabricated by a fully conventional photolithography process. The switching voltage between two

states is reduced, and a higher pixel on/off contrast is obtained due to the novel non-planar electrode design, pushing bistable EWDs a step closer to commercial application.

## 2 Methods

The design of a bistable EW device includes a non-planar electrode structure (Figs. 1a and 1b). Polar (water) and non-polar (colored oil) liquid media were sealed between the top and bottom glass plates. Separated thick dielectric steps (called “pixels”) were fabricated on the bottom glass plate, forming channels between pixels. Colored oil could stay stable either on the top of pixels or in channels, and the switching between two states was controlled by pixel electrodes (G1) and channel electrodes (G2). In our design, pixel electrodes were on the top of the thick dielectric step, i.e., high above the bottom glass plate. U-shaped channel electrodes were on the bottom glass plate directly with two wings, standing adjacent to the sidewall of pixels and extending to its upper edge.

The fabrication process of the non-planar electrode EW devices is shown in Figs. 1e–1j. A layer of SU-8 photoresist, about 20- $\mu\text{m}$  thick, was first spin-coated onto the bottom glass plate and then patterned into cuboids by photolithography. The cuboids served as the step dielectrics of pixels. To fabricate the pixel electrodes and channel electrodes, an 80-nm thick Al layer was deposited onto the substrate by magnetron sputtering. Then photoresist (Microposit S1813) was spin-coated and patterned. The exposed Al was wet etched, while the Al protected by photoresist was left untouched. After photoresist stripping, the control electrodes, G1 and G2, were obtained. To prevent electrolysis, control electrodes in the EW device were usually covered by a dielectric layer. In this study, an 800-nm thick  $\text{Si}_3\text{N}_4$  layer was grown by plasma enhanced chemical vapor deposition (PECVD) on the top of electrodes at 80 °C. Then a hydrophobic layer, CYTOP (Asahi CTL-809M), was spin-coated to yield an about 115-nm thick layer. The sample was then baked at 180 °C in a vacuum oven for 10 min to fully cure the SU-8 and to enhance the adhesion of the CYTOP layer. The devices were dosed underwater using a syringe filled with colored oil (dodecane with dissolved blue dye) which filled channels by capillary

action. The blue dye (Keystone AUTOMATE™ BLUE 8AHF) was purified before being dissolved in dodecane (Zhou et al., 2009). Finally, the bottom glass plate was sealed underwater using epoxy to a top glass plate with unpatterned indium tin oxide (ITO) as top electrodes.

For comparison, EW devices with a planar electrode structure, the same as that in Charipar et al. (2015), were fabricated (Figs. 1c and 1d). The pixel electrodes and channel electrodes were in the lowest layer on the bottom glass plate, and the dielectric steps were on the top of pixel electrodes. The fabrication process of the planar electrode EW devices was similar to that of the non-planar devices, as described above, except that in planar devices the pixel electrodes and channel electrodes were patterned before the SU-8 steps. Figs. 1k and 1l show the optical images fabricated by planar and non-planar electrodes, respectively.

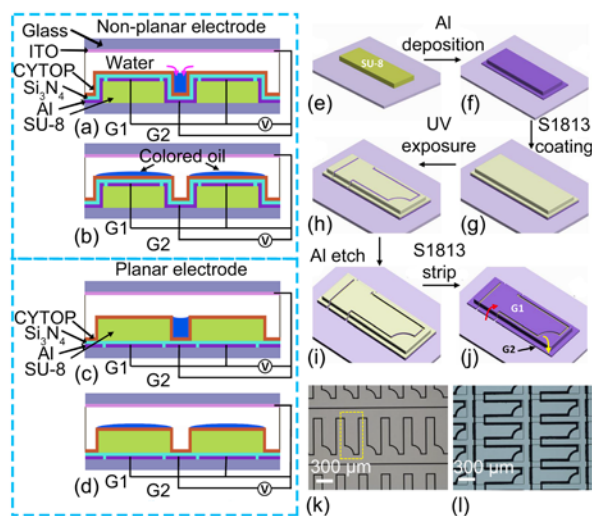


**Fig. 1** Schematic of the structure and working principle of the non-planar and planar bistable electrowetting devices: (a) non-planar device with a voltage applied to the pixel electrodes G1; (b) non-planar device with a voltage applied to the channel electrodes G2; (c) planar device with a voltage applied to the pixel electrodes G1; (d) planar device with a voltage applied to the channel electrodes G2; (e)–(j) fabrication process of the non-planar electrode structure; (k) an optical image of the fabricated planar electrode; (l) an optical image of the fabricated non-planar electrode

The red arrow in (j) indicates where the oil flows from the channel to the pixel, while the yellow arrow indicates the reverse case. The box area in (k) corresponds to the position of an SU-8 cuboid on the electrodes

### 3 Experimental results and discussion

Electrode fabrication is obviously the most critical part of the fabrication process of our non-planar designed EW devices. According to Fig. 1, both pixel electrodes and channel electrodes were designed to cross the about 20- $\mu\text{m}$  high SU-8 steps and remained isolated from each other. Thus, the Al film must cover the top surface of the SU-8 cuboids through its sidewall continuously down to the channel surface. To accomplish this, magnetron sputtering was chosen for Al deposition, as it was known for its ease of deposition on uneven surfaces. The electrodes were patterned by combining conventional photolithography and wet etching techniques. This is because we wanted to develop a fabrication process compatible with mass production of the non-planar bistable EW devices. Fabrication of non-planar electrode structures was quite routine in micro-electromechanical systems. However, it was challenging for us because of the lack of experience. To isolate the pixel electrodes and channel electrodes, photoresist should be patterned first for selective wet etching of the unwanted Al film area. To coat the photoresist all over the uneven surface, the S1813 photoresist was spin-coated at a relatively low speed, about 300 r/s. Fig. 2a shows the scanning electron microscope (SEM) images of the non-planar electrodes. A zoom-in SEM image at a corner of a pixel is shown in Fig. 2b, which confirms that the Al film was deposited continuously and uniformly across the high pixel steps. Figs. 2c and 2d show the Al etching results, demonstrating that the pixel and channel electrodes were successfully isolated in the pixels, channels, and sidewall areas. The electrical measurement confirmed the separation of pixel electrodes and channel electrodes. In contrast, patterning of planar metal electrodes was much easier by conventional lithography (Fig. 1k). The pixel and channel electrodes were isolated following the outline of the rectangular pixels, but had one corner notched off for both non-planar and planar designs (Figs. 1 and 2). This design helped guide the fluid off the pixel surface, as demonstrated in Charipar et al. (2015).

After CYTOP coating, the water contact angle on the hydrophobic surface was measured to be about 115°, which was good for EW operation (Zhang et al., 2017).

The oil was immersed in a water medium in an EW device, which wet the CYTOP surface. Since the

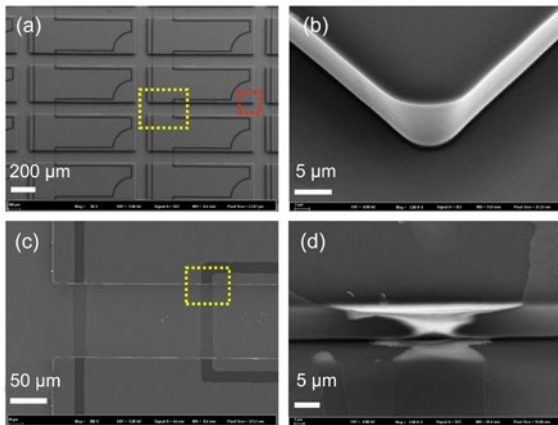


**Fig. 2** Fabrication results of non-planar electrodes: (a) an scanning electron microscope (SEM) image of the non-planar electrode structure; (b) a zoom-in SEM image of the red box area in (a), showing that Al was continuously deposited across the SU-8 step; (c) a zoom-in SEM image of the yellow box area in (a); (d) a zoom-in SEM image of the yellow box area in (c), showing that the pixel and channel electrodes were isolated on the sidewall of a pixel

entire surface of the bottom glass plate was covered with CYTOP (Fig. 1), the oil, when settled, was prevented from creeping along the device surface by the water/oil surface tension and remained stable irrespective of the surface it occupied (Charipar et al., 2015). However, the situation changed once an electric voltage was applied. The colored oil was initially dosed onto the channel area of the device by capillary force, and then settled down (Figs. 3a and 3a') due to the water/oil surface tension. Figs. 3b–3f' depict the switching process of the bistable states. Figs. 3b and 3b' correspond to the off-state of pixels, where oil stays stable on pixels without any voltage applied to the pixel and channel electrodes. Once a voltage was applied to the pixel electrodes (G1), water wet the pixels and pushed oil into the channels (Figs. 3c and 3c'). The pixels were switched to the on-state, and water remained stable when the voltage applied to G1 was removed (Figs. 3d and 3d'). When an operating voltage was applied to the channel electrodes (G2), the non-polar oil did not respond to the applied voltage, while water (polar medium) was pulled towards the bottom of channels. This pushed the oil out of channels to the pixel surface (Figs. 3e and 3e'). When the voltage was removed, the water remained in channels. This is because energy was required for the water to overcome the physical barrier at the edge of the pixel surface. After being pushed onto pixels,

the oil relaxed and spread over the pixel surface. As discussed before, the oil remained stable on the pixel surface without the applied voltage, and the pixels reached the stable off-state (Figs. 3f and 3f'). Thus, the oil could stay stable either in channels or on pixels, and the two states could be switched by the applied voltage. These results indicated that a bistable system was realized in the non-planar EW devices. Note that because there was residual oil on pixels, the on-states during the operation of devices (Figs. 3d and 3d') were not as good as the initial on-states (Figs. 3a and 3a'). This was caused by imperfections in devices, which should be improved in the future.

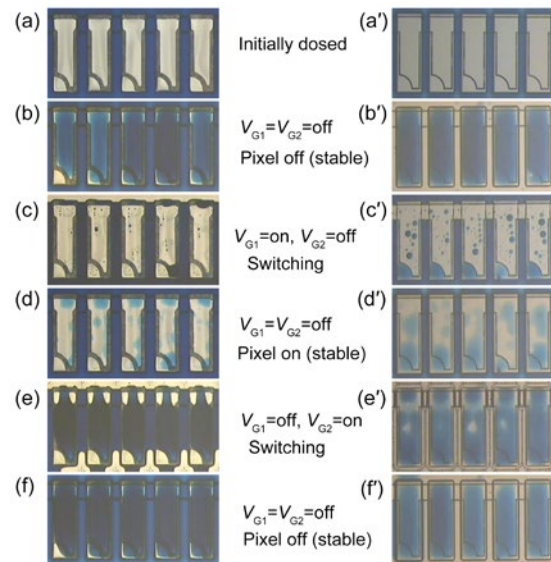


**Fig. 3** Optical images of the devices while switching between two stable states for non-planar (a–f) and planar (a'–f') electrowetting devices

Bistable operations were realized in both planar and non-planar devices (Fig. 3). However, the performances were different. The switching voltages of the planar designed devices were usually in the range of 70–140 V, while those of the non-planar devices were much lower in the range of 40–60 V. This was explained by the differences in the design of electrodes. In planar design, in addition to the  $\text{Si}_3\text{N}_4$  dielectric layer, the thick SU-8 on pixel electrodes and the non-polar oil layer on channel electrodes reduced the electric field that the water experienced at the interface. Thus, relatively high voltages were required for water to wet CYTOP and push the oil out of or into the channels. In non-planar design, the pixel electrodes were raised to the top of the SU-8 cuboids.

Therefore, the voltage required to drive the oil into channels was determined by only the thin  $\text{Si}_3\text{N}_4$  dielectric layer, and it was lower than that required by the planar device. In the case of driving oil from channels to pixels, water started to wet the CYTOP at the wing of the U-shaped channel electrodes when the voltage was applied, as shown by the magenta arrows in Fig. 1a. Then water was pulled down into channels along the wing as the voltage increased, and oil was pushed to pixels along the sidewall part of the pixel electrodes (as indicated by the red arrow in Fig. 1j). The required driving voltage was determined by the thin  $\text{Si}_3\text{N}_4$  dielectric layer according to Fig. 1a, which was lower than that of planar design. Fig. 3 confirms the advantages of non-planar electrode design.

The two stable states of the device corresponded to the on- and off-state of an EWD. The switching speed and contrast ratio between the on- and off-state were important parameters for a display. Unfortunately, we currently lacked appropriate equipment for measuring such parameters. However, we attempted to gain some information about these properties. The bistable operation of the non-planar EWDs was recorded by an accessory CCD camera of an optical microscope. Then the recorded images were analyzed frame by frame to obtain the switching speed. The average brightness of the pixel area was extracted from the frame images, so that the on/off contrast ratio could be estimated. Fig. 4 shows the extracted brightness changes during the successive switching by voltage pulses. Once a voltage pulse was applied to channel electrodes, oil in channels beaded up transiently causing a spike in brightness, and a certain volume of oil was pushed onto pixels. This switching was completed between two single frames of the video for some pixels, which corresponded to the switching time less than 40 ms (25 frames/s). These results demonstrated that our non-planar EW devices has potential for video speed display applications.

When the applied voltage was removed, the oil drop immediately relaxed on the pixel surface, resulting in a sharp decrease in brightness and then a gradual decay to a stable value. The total volumes of the oil pushed onto pixels depended on the number of voltage pulses applied to channel electrodes, causing a step change in the average pixel brightness (Fig. 4).

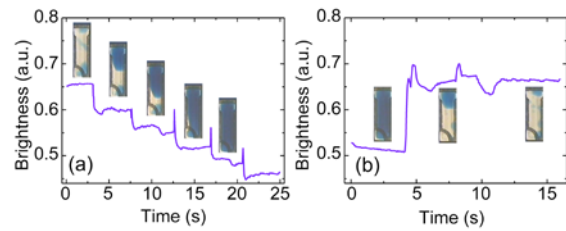


**Fig. 4 Pixel brightness changes when it is switched off (a) and on (b)**

The spike was not captured for some pulses which were too fast. Insets are images of pixels when the oil was relaxed

These indicated that the gray scale of pixels could be tuned by the voltage applied to G2 with an appropriate wave form. Corresponding results from the reverse switching are shown in Fig. 4b, where a sharp increase of brightness was observed with a similar switching speed. The contrast ratio was estimated by the extracted maximum darkness and brightness of the two stable states, and 10%–20% improvement was observed for the non-planar device compared with the planar device. A rough estimation of the contrast ratio confirmed that the non-planar devices had a higher contrast ratio than the planar devices. This could be easily confirmed from Fig. 3. We believed the difference in the on/off contrast ratio was due to the design of devices. The thick SU-8 cuboids (with a relatively low dielectric constant) on pixel electrodes in planar design were relocated under pixel electrodes in non-planar design. Therefore, the dielectric layers on both pixel electrodes and channel electrodes were thin and uniform, and had a high dielectric constant. These factors strengthened the electric field exerted on the liquid, and lowered the switching voltage. According to the thickness and dielectric constant of the dielectric layer used in two designs, the estimated switching voltage of planar design should be about 4–5 times that of non-planar design (Verheijen and Prins, 1999), which was roughly consistent with our experimental results. Since the required voltage to drive the oil from pixels to channels for the planar device was much higher than that of the non-planar device, there was usually more residual oil on pixels of the planar device, which lowered the brightness of the on-state (Figs. 3c, 3c', 3d, and 3d'). Charipar et al. (2015) proposed that the driving voltage of the planar device could be lowered by reducing the SU-8 thickness. However, a thinner SU-8 led to a shallower channel and a smaller volume

of dosed oil, thus reducing the darkness of the off-state and lowering the on/off contrast. Though a wider channel could store more colored oil and was helpful for pixel contrast, the pixel aspect ratio was compromised. These problems were easily solved by non-planar device design, where the driving voltage was determined mainly by the thickness of the  $\text{Si}_3\text{N}_4$  dielectrics. Thus, a very deep channel was applicable, which would benefit the darkness of the off-state and the on/off contrast without compromising the aspect ratio.

The concept of a non-planar bistable EW device is demonstrated in this study. However, a lot of work is needed to complement this idea. The fabrication process should be optimized. For example, photoresist is spin-coated onto the thick structures on the bottom glass plate at a low speed. Though it can be coated on the full surface, the thickness of S1813 is not uniform, especially at the corner of pixels, causing difficulties for ultraviolet (UV) exposure and development. Therefore, we doubled the exposure dose to fully expose the photoresist. However, this overdose exposure causes the obtained etching width to be larger than that of the design. This will have an impact on the patterning results of the electrodes and on the performance of the fabricated devices. Sometimes, we find that the isolation between pixel and channel electrodes is unsuccessful, leading to device failures. This problem can be solved by dip coating, which is used for uniformly coating photoresist on uneven surfaces (Brinker, 2013). A dip coater has been ordered, so that both photoresist and CYTOP can be uniformly coated in our future fabrications. We believe this will improve the device performance and fabrication yield. Though the switching time is less than 40 ms, we still observed longer switching time (about 100 ms) in some pixels. This indicates that the uniformity of our device should be improved. Moreover, the oil can be quickly pushed onto pixels. The oil droplet relaxes slowly, and the pixel gray scale is related to the number of voltage pulses. Therefore, three or four successive pulses are used to switch the pixel on- and off-state to the gray scale. These results indicate that the operating voltage signal should be optimized, e.g., using a high frequency (kHz) wave. Future work is to improve the overall performance of our bistable EW device to address all these concerns.

## 4 Conclusions

In this study, we have fabricated a bistable EW device with non-planar controlling electrodes through a fully conventional lithographic process, and have demonstrated its potential for low power display applications. Due to the novel non-planar design, the switching voltage has been reduced and the contrast ratio improved compared with the bistable EWs with planar electrodes previously reported. These achievements strengthen our work on bistable EW devices and lay a solid foundation for future development.

### Compliance with ethics guidelines

Han ZHANG and Xue-lei LIANG declare that they have no conflict of interest.

### References

- Bitman A, Bartels F, Rawert J, et al., 2012. Production considerations for bistable droplet driven electrowetting displays. Society for Information Display Int Symp, p.1-4. <https://doi.org/10.1002/j.2168-0159.2012.tb05918.x>
- Blankenbach K, Schmoll A, Bitman A, et al., 2008. Novel highly reflective and bistable electrowetting displays. *J Soc Inform Disp*, 16(2):237-244. <https://doi.org/10.1889/1.2841856>
- Blankenbach K, Jentsch M, Rawert J, et al., 2011. Sunlight readable bistable electrowetting displays for indicators and billboards. Society for Information Display Int Symp, p.1-4. <https://doi.org/10.1889/1.3621150>
- Brinker CJ, 2013. Dip coating. In: Schneller T, Waser R, Kosec M, et al. (Eds.), Chemical Solution Deposition of Functional Oxide Thin Films. Springer, Vienna, p.233-261.
- Charipar KM, Charipar NA, Bellemare JV, et al., 2015. Electrowetting displays utilizing bistable, multi-color pixels via laser processing. *J Disp Technol*, 11(2):175-182. <https://doi.org/10.1109/JDT.2014.2364189>
- Chen CY, Wang CY, Wang WC, et al., 2011. A 3.5-inch bendable active matrix electrowetting display. Society for Information Display Int Symp, p.1-4. <https://doi.org/10.1889/1.3621328>
- Cho SK, Moon H, Kim CJ, 2003. Creating, transporting, cutting, and merging liquid droplets by electrowetting-based actuation for digital microfluidic circuits. *J Microelectromech Syst*, 12(1):70-80. <https://doi.org/10.1109/JMEMS.2002.807467>
- Comiskey B, Albert JD, Yoshizawa H, et al., 1998. An electrophoretic ink for all-printed reflective electronic displays. *Nature*, 394(6690):253-255. <https://doi.org/10.1038/28349>
- Dai YX, 2008. Design and Operation of TFT LCD Panels. Tsinghua University Press, Beijing, China (in Chinese).

- Deng Y, Tang B, Henzen AV, et al., 2017. Recent progress in video electronic paper displays based on electro-fluidic technology. Society for Information Display Int Symp, p.1-4. <https://doi.org/10.1002/sdtp.11695>
- Hayes RA, Feenstra BJ, 2003. Video-speed electronic paper based on electrowetting. *Nature*, 425(6956):383-385. <https://doi.org/10.1038/Nature01988>
- Heikenfeld J, Zhou K, Kreit E, et al., 2009. Electrofluidic displays using Young-Laplace transposition of brilliant pigment dispersions. *Nat Photon*, 3(5):292-296. <https://doi.org/10.1038/Nphoton.2009.68>
- Hou L, Smith NR, Heikenfeld J, 2007. Electrowetting manipulation of any optical film. *Appl Phys Lett*, 90(25):1-3. <https://doi.org/10.1063/1.2750544>
- Huh D, Tkaczyk AH, Bahng JH, et al., 2003. Reversible switching of high-speed air-liquid two-phase flows using electrowetting-assisted flow-pattern change. *J Am Chem Soc*, 125(48):14678-14679. <https://doi.org/10.1021/ja037350g>
- Jones TB, 2005. An electromechanical interpretation of electrowetting. *J Micromech Microeng*, 15(6):1184-1187. <https://doi.org/10.1088/0960-1317/15/6/008>
- Jung HY, Choi UC, Park SH, et al., 2012. Development of driver IC with novel driving method for the electrowetting display. Society for Information Display Int Symp, p.1-4. <https://doi.org/10.1002/j.2168-0159.2012.tb06022.x>
- Kuiper S, Hendriks BHW, 2004. Variable-focus liquid lens for miniature cameras. *Appl Phys Lett*, 85(7):1128-1130. <https://doi.org/10.1063/1.1779954>
- Lao Y, 2008. Ultra-High Transmission Electrowetting Displays. MS Thesis, University of Cincinnati, Cincinnati, USA.
- Mugele F, Baret JC, 2005. Electrowetting: from basics to applications. *J Phys Condens Matter*, 17(28):705-774. <https://doi.org/10.1088/0953-8984/17/28/R01>
- Pollack MG, Shenderov AD, Fair RB, 2002. Electrowetting-based actuation of droplets for integrated microfluidics. *Lab Chip*, 2(2):96-101. <https://doi.org/10.1039/b110474h>
- Rawert J, Jerosch D, Blankenbach K, et al., 2010. Bistable D<sup>3</sup> electrowetting display products and applications. Society for Information Display Int Symp, p.1-4. <https://doi.org/10.1889/1.3500404>
- Shui LL, Hayes RA, Jin ML, et al., 2014. Microfluidics for electronic paper-like displays. *Lab Chip*, 14(14):2374-2384. <https://doi.org/10.1039/c4lc00020j>
- Smith NR, Abeysinghe DC, Haus JW, et al., 2006. Agile wide-angle beam steering with electrowetting micropisms. *Opt Expr*, 14(14):6557-6563. <https://doi.org/10.1364/Oe.14.006557>
- Verheijen HJJ, Prins MWJ, 1999. Reversible electrowetting and trapping of charge: model and experiments. *Langmuir*, 15(20):6616-6620. <https://doi.org/10.1021/la990548n>
- Yang S, Zhou K, Kreit E, et al., 2010. High reflectivity electrofluidic pixels with zero-power grayscale operation. *Appl Phys Lett*, 97(14):1-3. <https://doi.org/10.1063/1.3494552>
- You H, Steckl AJ, 2010. Three-color electrowetting display device for electronic paper. *Appl Phys Lett*, 97(2):1-3. <https://doi.org/10.1063/1.3464963>
- Zhang H, Yan QP, Xu QY, et al., 2017. A sacrificial layer strategy for photolithography on highly hydrophobic surface and its application for electrowetting devices. *Sci Rep*, 7(1):1-7. <https://doi.org/10.1038/s41598-017-04342-z>
- Zhou K, Heikenfeld J, Dean KA, et al., 2009. A full description of a simple and scalable fabrication process for electrowetting displays. *J Micromech Microeng*, 19(6):1-12. <https://doi.org/10.1088/0960-1317/19/6/065029>